

BERENIKA HAUSNEROVA<sup>\*)</sup>, NATALIE HONKOVA, ANEZKA LENGALOVA,  
TAKESHI KITANO, PETR SAHA

Tomas Bata University in Zlín  
Faculty of Technology  
Polymer Centre  
T. G. Masaryka 275, 762 72 Zlín, Czech Republic

## Rheological behavior of fibre-filled polymer melts at low shear rate

### Part II. EXPERIMENTAL INVESTIGATION<sup>\*\*)</sup>

**Summary** — In this study, rheological properties of carbon fibre-filled polypropylene and polyethylene melts at low shear rate were measured using a cone-plate rheometer. The melts with high fibre loading show complex shear flow depending on the fibre concentration, its length and length distribution, as well as on shear rate and matrix characteristics. The existence of yield stress and time-dependent or shear-strain-dependent properties are also discussed and compared with previous results. The shear flow in the narrow gap of cone-plate rheometer influences the fibre assembly. However, the effect of low shear rate on the structure of fibre assembly is negligible.

**Key words:** polymer melt, polypropylene, polyethylene, carbon fibres, rheological properties.

CHARAKTERYSTYKA REOLOGICZNA W ZAKRESIE NISKICH SZYBKOŚCI ŚCINANIA STOPÓW POLIMERÓW NAPEŁNIONYCH WŁÓKNAMI. Cz. II. BADANIA EKSPERYMENTALNE

**Streszczenie** — Zbadano właściwości reologiczne stopów polipropylenu i polietylenu napełnionych włóknami węglowymi w ilości do 20 % obj. Pomiaru wykonano za pomocą reometru stożek-platek w zakresie niskich szybkości ścinania. Stopy o wysokim stopniu napełnienia wykazywały złożony charakter zależności przepływu ścinającego od zawartości włókien, ich długości i rozkładu długości oraz od szybkości ścinania i właściwości matrycy polimerowej. Zbadano i przedyskutowano właściwości zależne od czasu i odkształcenia przy ścinaniu oraz występowanie granicy plastyczności porównując wyniki z uzyskanymi wcześniej. Tarcie podczas przepływu stopu przez szczelinę między stożkiem a płytką reometru wpływa na zespoły włókien, ale wpływ szybkości ścinania (w badanym zakresie) na strukturę tych związków jest zaniedbywalny.

**Słowa kluczowe:** stop polimeru, polipropylen, polietylen, włókna węglowe, właściwości reologiczne.

In paper [1] we described the models applied for the description of fibre filled non-Newtonian liquids under low shear rates.

The present paper describes experimental results on rheological behavior of short fibre-filled polymer melts, mainly at low shear rate region. Rheological properties, such as shear viscosity, time-dependent flow properties, yield stress and shear modulus of carbon fibre-filled polymer melts were measured. Two types of polymers, polyethylene and polypropylene were used as matrixes, and the effects of fibre loading, fibre length and its distribution, and shear rate on the flow properties were followed.

### EXPERIMENTAL

#### Materials

Two types of low-density polyethylene (PE-1, Flowthene G701N,  $MFR = 7.8$ , and PE-2, Flowthene G401,

$MFR = 4$ , powders, manufactured by Seitetsu Chemical Ind. Co.), and two types of polypropylene, one of which was compounded in two different ways, giving two materials (PP-1 and PP-2, Sumitomo NOBLEN W101, pellets, Sumitomo Chemicals Co.), and the other (PP-3, PN670, powder,  $MFR = 23$ , Tokuyama Co.) were used as matrixes for fibre-filled systems. As the filler, carbon fibre (CF) from Toho Rayon Co. (Beshight, diameter 7  $\mu\text{m}$ , 3 mm chopped strand) was used.

#### Compounding procedures

Two methods described below were used for melt mixing of the fibres with polymers.

All the compounding processes were carried out at the temperature of 200 °C in the melting zone.

<sup>\*)</sup> Corresponding author; e-mail: hausnerova@ft.utb.cz

<sup>\*\*)</sup> Part I — see [1].

### Compounding in a single-screw extruder

Weighed amounts of PE-1 or PP-3 and the fibres (chopped strand) were mixed in a single-screw extruder (screw  $D = 25$  mm,  $L = 20D$ , Union Plastics Co.) at a screw rotation speed of 80 rpm. For PP-1, a single-screw extruder ( $D = 19$  mm,  $L = 20D$ , Plasticorder PLV151, Brabender Co.) was used with the screw speed of 25 rpm.

Four kinds of carbon fibre-filled systems were mixed, differing in volume fraction (up to 20 vol. %). The extrudate was cooled in a water bath, cut on a pelletizer into pellets about 5 mm long and dried in an air oven. The pellets were extruded two more times so that well dispersed fibre structure could be obtained.

### Compounding in a twin-screw extruder

A combination of a single-screw extruder (Bus-Kneader, PR46,  $D = 46$  mm,  $L = 11D$ ), and a twin-screw extruder (counter rotation, Werner Pfleiderer, ZKS 30M,  $D = 30$  mm,  $L = 20D$ ) was used to compound a matrix polymer PE-2 with fibres. The samples were pre-compounded in the single-screw extruder at the highest concentration (20 vol. %) before being subjected to final compounding in the twin-screw extruder. In the latter operation, samples with lower concentrations were obtained by addition of pure matrix material. This technique resulted in a fibre length distribution almost independent on the fibre concentration.

For the compounding of PP-2 with fibres, a twin-screw extruder ( $D = 35$  mm,  $L = 15D$ , counter-rotation, RT35-2S, Tsukada Juki Co.) was used with the screw speed of 25 rpm. The process of preparation of pellets

after extrusion was the same as in the case of the single-screw extruder. Four kinds of systems with different volume fraction were prepared also in this process.

### Sample preparation and characterization

The pellets prepared by each method were compression-molded at 200 °C and 5 MPa into a sheet 3 mm thick. Test samples for the rheological measurements were cut from this sheet in the shape of about 30 mm diameter discs.

The fibre content (weight fraction) was determined gravimetrically after incineration of matrix materials. The volume fraction ( $\Phi$ ), of the fibre at the test temperature was calculated from the densities of the components at this temperature.

**Table 2.** Zero shear viscosities of the matrices at 200 °C

Type of polymer matrix	$\eta_0$ , Pa · s
PE-1	2100
PE-2	2800
PP-1	6000
PP-2	3800
PP-3	5000

To determine the fibre length distribution the incineration residue was immersed in water and filaments were dispersed carefully. They were spread on a glass plate, and after removing water the overall feature was

**Table 1.** Characteristics of the samples

Symbol of sample	Volume fraction of fibre $\Phi$ , %	Number average fibre length ( $l_N$ ), mm	Weight average fibre length ( $l_W$ ), mm	$l_W/l_N$	Number average aspect ratio [ $(a_r)_N$ ]	Method
CF5/PE-1	4.4	0.460	0.653	1.42	66	S
CF10/PE-1	8.8	0.386	0.564	1.46	55	
CF15/PE-1	12.3	0.298	0.413	1.38	43	
CF20/PE-1	16.6	0.240	0.292	1.22	34	
CF5/PE-2	5.6	0.200	0.234	1.17	29	S/T
CF10/PE-2	10.4	0.193	0.221	1.15	28	
CF15/PE-2	12.9	0.189	0.216	1.14	27	
CF20/PE-2	18.3	0.192	0.203	1.06	27	
CF5/PP-1	5	0.447	0.666	1.49	64	S
CF10/PP-1	10	0.387	0.581	1.50	51	
CF15/PP-1	15	0.202	0.310	1.53	29	
CF20/PP-1	20	0.206	0.326	1.58	29	
CF5/PP-2	5	0.334	0.442	1.32	48	T
CF10/PP-2	10	0.325	0.411	1.27	47	
CF15/PP-2	15	0.273	0.344	1.26	39	
CF20/PP-2	20	0.225	0.281	1.25	32	
CF5/PP-3	4.8	0.335	—	—	48	S
CF10/PP-3	9	0.303	—	—	43	
CF15/PP-3	15.3	0.238	—	—	34	
CF20/PP-3	24	0.169	—	—	24	

S — single-screw extruder. T — twin-screw extruder.

photomicrographed. From the photograph the length of each filament was measured and the distribution of the fibre lengths in the test sample was determined.

Table 1 shows the characteristics of carbon fibre-filled systems, *i.e.*  $\Phi$ , number average length ( $l_N$ ), weight average length ( $l_W$ ), their ratio, number average aspect ratio [ $(a_r)_N$  defined as  $l_N/d$ , where  $d$  is the fibre diameter] of the filler, and also the compounding method for each system. Zero-shear viscosities ( $\eta_0$ ) of matrices at 200 °C are given as well in Table 2.

### Rheological measurements

Rheological properties of the fibre-filled polymer melts were measured using a cone-plate rheometer (151-S, Nippon Rheology Kiki Co.) with the cone radius 2.15 cm and angle 4°; the cone was truncated at the tip by 200  $\mu\text{m}$ . All the measurements were performed at 200 °C. Ordinary steady shear flow measurements were carried in the range of shear rates  $5 \cdot 10^{-3}$  to  $10 \text{ s}^{-1}$ .

For the samples with high fibre loading, time-dependent shear stress at the lowest shear rates approaches to a steady value only very slowly, and quite a long time (tens of minutes to an hour) is often needed to achieve a steady state; sometimes it is difficult to obtain the steady value at all. Two different test procedures (denoted A and B) were chosen, one for the determination of transient shear flow at low rates, and the other for steady shear flow measurements.

Both procedures were applied to all samples.

In procedure A the time-dependent shear stress or stress growth in the system was measured (Figure 1a).

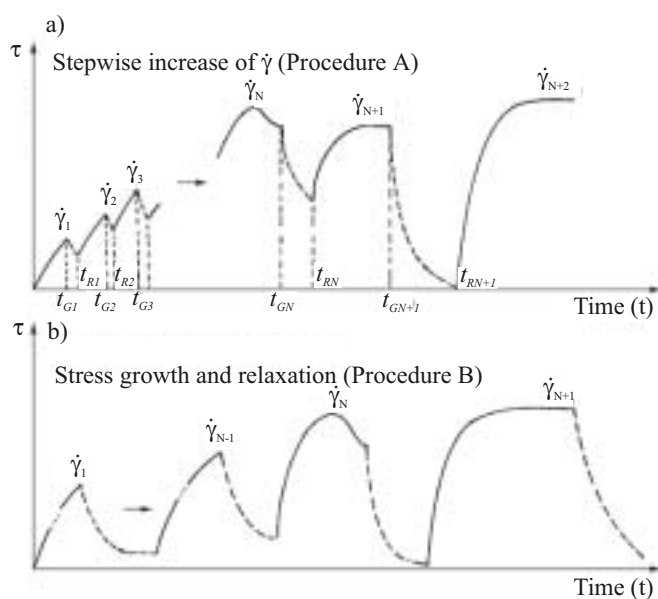


Fig. 1. Test procedures for transient and steady shear flow properties of fibre-filled polymer system: a) procedure A — transient shear flow properties under stepwise change of shear rate; b) procedure B — steady shear flow properties, stress growth and relaxation measurements

Shear rate was changed stepwise after stress /shear strain growth, and then the flow was stopped and the stress in the sample was partially relaxed. Generally, for a highly loaded sample it is difficult to relax the shear stress completely because of its long relaxation time or the existence of the yield stress. After some relaxation (the amount of relaxation was not fixed) the rheometer was started again. The processes continued with stepwise increase in shear rate. Shear stress as a function of time under constant shear rate was measured during the time longer than 30 s. This time interval became longer exponentially with the decrease in shear rate. At a critical shear rate, time dependent shear stress began to decrease after reaching a maximum. This behavior was observed only for polyethylene-based samples with high fibre content, as will be shown later. Shear stress as a function of time or strain was recorded.

The other type of tests, called Procedure B, was an ordinary shear stress growth and relaxation experiment, as shown in Figure 1b. At relatively high shear rate, we could obtain steady shear stress after its growth, and also the shear stress relaxed almost to zero even for high content of fibre in the system.

### RESULTS AND DISCUSSION

In the following, transient and steady shear flows will be discussed separately after the characterization of the fibres in the tested materials.

#### Fibre length and distribution in the samples

As can be seen from Table 1,  $l_N$  and  $(a_r)_N$ , generally decrease as fibre loading increases. The changes of  $l_N$  with fibre loading are larger for the samples compounded in single-screw extruder than for those mixed in twin-screw extruder. It is known from earlier investigations [2] that the fibre length distribution of CF in the samples prepared in single-screw extruder becomes narrower with increasing fibre loading, and, on the other hand, the length distributions of the fibres in the samples prepared in twin-screw extruder are nearly the same irrespective of fibre loading.

#### Transient shear flow behavior

Figure 2 shows the results for two CF/PE-1 samples with the lowest and highest filling (CF5 and CF20) measured according to procedure A. Shear stress ( $\tau$ ), versus shear strain ( $\epsilon$ ) [which is the product of shear rate ( $\dot{\gamma}$ ), and time ( $t$ )] curves are shown in double logarithmic coordinates for  $\dot{\gamma}$  increased in a stepwise manner. For simplicity, the figure only shows some of the values of shear rates measured in the experiments.

As can be seen, at very low  $\dot{\gamma}$  (different values)  $\tau$  increases monotonously with rising  $\epsilon$ , and single curves under different  $\dot{\gamma}$  are obtained for both samples. At a

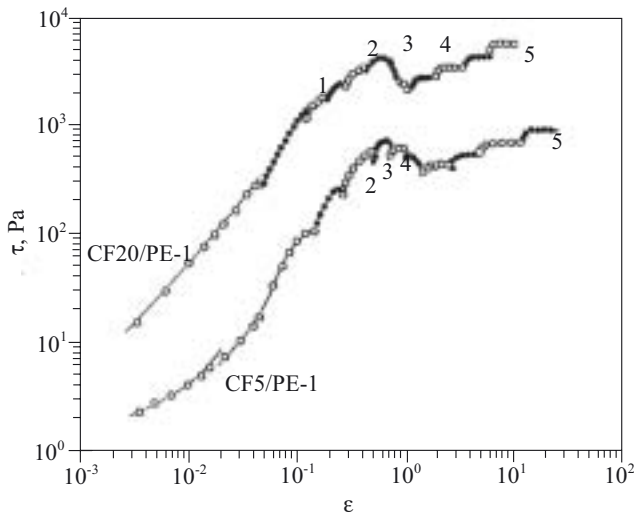


Fig. 2. Relationship between shear stress ( $\tau$ ) and shear strain ( $\epsilon$ ) for CF5/PE-1 and CF20/PE-1 samples (procedure A) dependent on shear rate ( $\dot{\gamma}$ ): 1 —  $0.00068 \text{ s}^{-1}$ , 2 —  $0.00159 \text{ s}^{-1}$ , 3 —  $0.00311 \text{ s}^{-1}$ , 4 —  $0.00614 \text{ s}^{-1}$ , 5 —  $0.0675 \text{ s}^{-1}$

critical  $\epsilon$ , however,  $\tau$  shows a maximum, then it slightly decreases and levels off. With a small increase in  $\dot{\gamma}$ ,  $\tau$  shows a monotonous increase and then has a constant value hereafter. From this behavior it can be said that steady shear flow properties can be measured quite reliably above the critical value.

Similar  $\tau$  vs.  $\epsilon$  behavior was observed for all CF/PE-1 samples. The critical  $\epsilon$  value, *i.e.* the region where  $\tau$  has a maximum, is around 0.8 for all samples. The figure also indicates that in lower  $\epsilon$  region these systems deform as an elastic materials. The shear modulus ( $G$ ), of the samples can be easily determined from the slope of the curves.

CF/PE-2 systems showed the properties similar to those of CF/PE-1 (not shown here) however, for these samples the critical  $\epsilon$  is smaller (about 0.4). We could not observe a critical point for CF5/PE-2 sample clearly as that of CF20/PE-2 sample. It was found from these results that the strain in which  $\tau$  has a maximum value seems to increase with the decrease in fibre content for both CF/PE-1 and CF/PE-2 systems.

The typical results of  $\tau$  growth measurements (procedure B) are shown for CF/PE-2 system (CF5 and CF20) in Figure 3. The relationship between time-dependent  $\tau$  and  $\epsilon$  strain ( $\epsilon = \dot{\gamma} t$ ) is shown at various shear rates in double-logarithmic coordinates. For CF20/PE-2 sample, the curves at  $\dot{\gamma}$  equal  $0.00023 \text{ s}^{-1}$  (symbol  $\bullet$ ) and  $0.00156 \text{ s}^{-1}$  (symbol  $\blacktriangle$ ) (no flow at both  $\dot{\gamma}$ ) exist at higher position than the curve of higher shear rate  $\dot{\gamma} = 0.0225 \text{ s}^{-1}$  (symbol  $\blacksquare$ ), when the material flows. These results coincide well with those obtained in step-wise experiments, and also  $\dot{\gamma}$  value at which the change of the  $\tau$  curve slope occurs coincides well with the other type of measurements. For CF5/PE-2 sample in the same figure, the stress overshoot phenomenon can be observed at  $\dot{\gamma} = 0.159 \text{ s}^{-1}$ , and

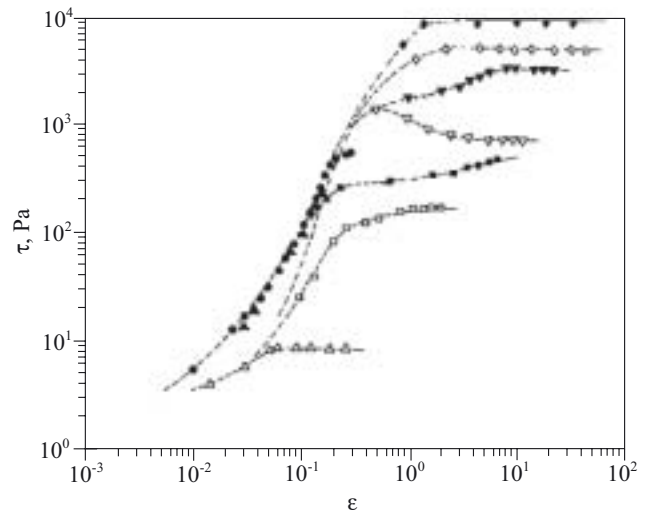


Fig. 3. Relationship between  $\tau$  and  $\epsilon$  for CF5/PE-2 (open symbols) and CF20/PE-2 (solid symbols) samples (procedure B) dependent on  $\dot{\gamma}$ :  $\bullet$  —  $0.00023 \text{ s}^{-1}$ ,  $\triangle, \blacktriangle$  —  $0.00156 \text{ s}^{-1}$ ,  $\square, \blacksquare$  —  $0.0225 \text{ s}^{-1}$ ,  $\nabla, \blacktriangledown$  —  $0.159 \text{ s}^{-1}$ ,  $\diamond, \blacklozenge$  —  $2.25 \text{ s}^{-1}$

steady shear stress increases monotonously with the rising  $\dot{\gamma}$ .

Generally, for all CF/PE-1 systems it was difficult to obtain  $\dot{\gamma}$  growth curves at  $\dot{\gamma}$  lower than  $0.003 \text{ s}^{-1}$ . From the results obtained in two types of time-dependent shear stress measurements for CF/PE-1 and CF/PE-2 systems, it can be said that highly loaded materials clearly show a yield stress which corresponds to the critical point where elastic deformation changes to plastic flow, and that  $G$  of the sample before the flow begins can be determined from the slope of  $\tau$  growth curve.

The samples based on polypropylene, on the other hand, showed behavior very different from CF/PE sys-

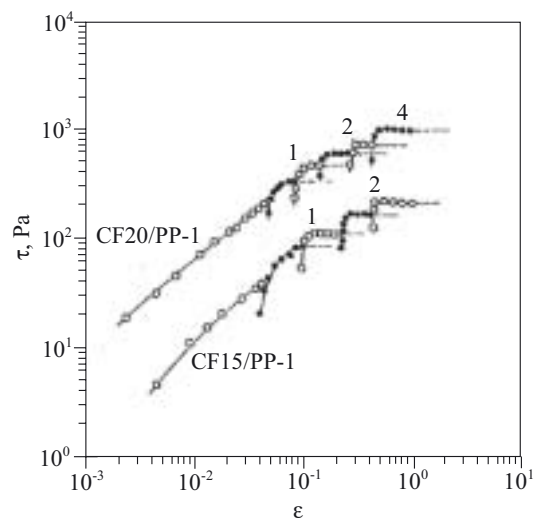


Fig. 4. Relationship between  $\tau$  and  $\epsilon$  for CF15/PP-1 and CF20/PP-1 samples (procedure A) dependent on  $\dot{\gamma}$ : 1 —  $0.00068 \text{ s}^{-1}$ , 2 —  $0.00159 \text{ s}^{-1}$ , 3 —  $0.00311 \text{ s}^{-1}$ , 4 —  $0.00614 \text{ s}^{-1}$



tems described above. An example of the data measured by procedure A (CF/PP-1 systems) is shown in Figure 4. The curves present the behavior of CF20/PP-1 and CF15/PP-1 samples. In the low strain region,  $\tau$  increases linearly with rising  $\varepsilon$ , and  $\tau$  values are obtained even at the shear rate of  $0.00068 \text{ s}^{-1}$  for both samples, but the  $\tau$  behavior appeared in CF/PE-1 and CF/PE-2 cannot be observed for this system, even at low  $\varepsilon$ . Steady shear stress can be determined easily from the low to high shear rate region. Similar results were obtained for the other CF/PP systems (CF/PP-1 and CF/PP-3).

The behavior of CF5/PP-1 and CF20/PP-1 under procedure B is depicted in Figure 5. As can be seen, for both samples  $\tau$  grows monotonously when  $\varepsilon$  increases, and the magnitude of the strain in which shear flow becomes steady depends on  $\dot{\gamma}$ . Again yield stress and stress overshoot were not observed for these systems, similarly as for the other polypropylene-based materials.

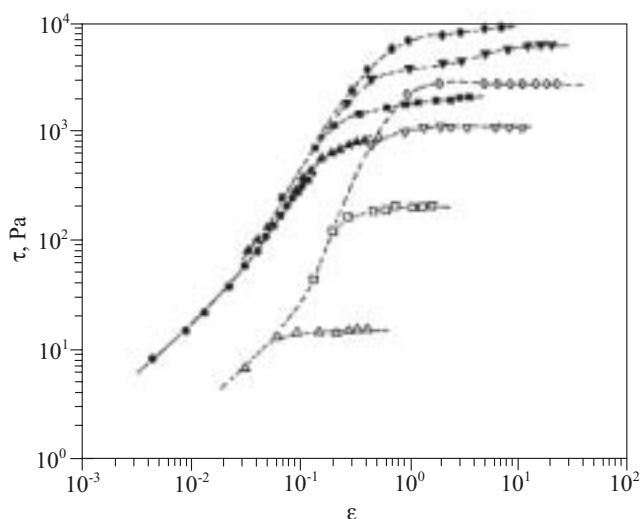


Fig. 5. Relationship between  $\tau$  and  $\varepsilon$  for CF5/PP-1 (open symbols) and CF20/PP-1 (solid symbols) samples (procedure B) dependent on  $\dot{\gamma}$ :  $\bullet$  —  $0.00023 \text{ s}^{-1}$ ,  $\triangle$ ,  $\blacktriangle$  —  $0.00159 \text{ s}^{-1}$ ,  $\square$ ,  $\blacksquare$  —  $0.0225 \text{ s}^{-1}$ ,  $\nabla$ ,  $\blacktriangledown$  —  $0.159 \text{ s}^{-1}$ ,  $\diamond$ ,  $\blacklozenge$  —  $0.917 \text{ s}^{-1}$

It is not so easy to understand the reason of the significant difference in time-dependent rheological properties between CF/PE and CF/PP systems. It is assumed that the differences in fibre lengths and their distributions do not affect the flow behavior so largely. Neither it is considered that the structures of fibre assemblies can cause the large difference in the two polymers flow.

When we compare the growths of shear stress and first normal stress difference of pure PE and PP melts at various  $\dot{\gamma}$ , we can observe a clear difference in time dependent curves [2, 3]. These differences of rheological properties of the matrix polymers may be one of the reasons for the distinct behavior of the CF-filled systems. It is worth saying that pure polymer transient flow proper-

ties can be predicted using some constitutive equations [4].

### Steady shear flow properties and yield stress

As shown in the Part I [1], measurements of steady shear flow properties of CF-filled PE systems at very low shear rates are more difficult compared to those of CF/PP systems. In the following we concentrate on typical results of procedure B (steady state shear flow) obtained for systems with both types of matrices, PE and PP.

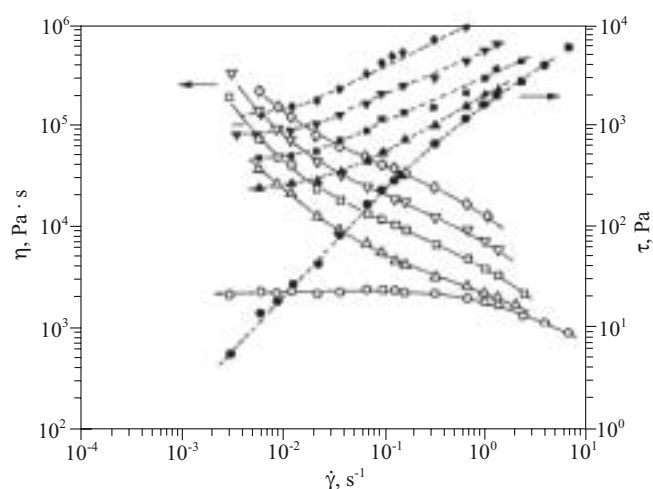


Fig. 6. Shear viscosity ( $\eta$ ) (open symbols) and  $\tau$  (solid symbols) curves vs.  $\dot{\gamma}$  for samples with PE-1 matrices:  $\circ$ ,  $\bullet$  — PE-1,  $\triangle$ ,  $\blacktriangle$  — CF5/PE-1,  $\square$ ,  $\blacksquare$  — CF10/PE-1,  $\nabla$ ,  $\blacktriangledown$  — CF15/PE-1,  $\diamond$ ,  $\blacklozenge$  — CF20/PE-1

Figure 6 shows the relationship among shear viscosity ( $\eta$ ),  $\tau$  and  $\dot{\gamma}$  for CF/PE-1 systems with various fibre contents. The matrix polymer shows Newtonian viscosity at the low  $\dot{\gamma}$  region, on the other hand, for the filled materials  $\eta$  decreases with rising  $\dot{\gamma}$  with quite a high slope (nearly  $-1$ ). The  $\tau$  values tend level off or have a plateau region with the decrease in  $\dot{\gamma}$ . This behavior indicates the existence of yield stresses; however, it is difficult to obtain stable data at  $\dot{\gamma}$  lower than  $5 \cdot 10^{-3} \text{ s}^{-1}$  for the reason mentioned in the previous section. Similar results were obtained for CF/PE-2 systems.

The flow properties of the other type of matrix are depicted in Figure 7 (CF/PP-1 systems). Compared to the flow curves of CF/PE-1 material shown in the previous figure, the measurements of  $\eta$  under steady shear flow are possible to be done at very low  $\dot{\gamma}$  values, around  $5 \cdot 10^{-4} \text{ s}^{-1}$ , which is almost one order of magnitude lower than for CF/PE systems. The other PP-based materials behaved alike.

Figure 8 presents the dependence of  $\eta$  on  $\tau$ , in fact re-plotted data from Figure 6 (for CF/PE-1, open symbols) and Figure 7 (for CF/PP-1, solid symbols) for dif-

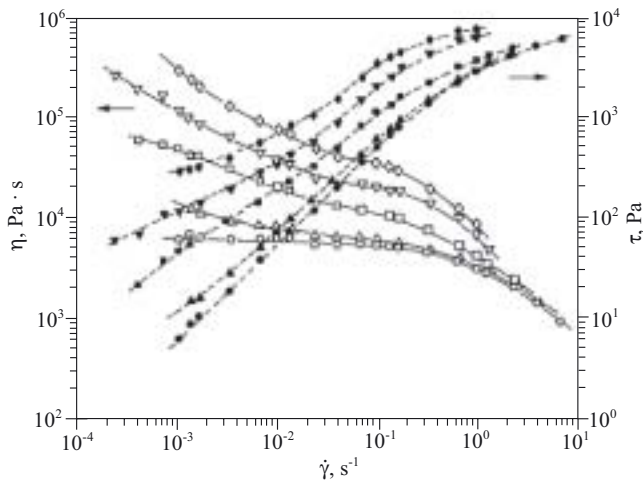


Fig. 7.  $\eta$  (open symbols) and  $\tau$  (solid symbols) curves vs.  $\dot{\gamma}$  for samples with PP-1 matrices:  $\circ, \bullet$  — PP-1,  $\triangle, \blacktriangle$  — CF5/PP-1,  $\square, \blacksquare$  — CF10/PP-1,  $\nabla, \blacktriangledown$  — CF15/PP-1,  $\diamond, \blacklozenge$  — CF20/PP-1

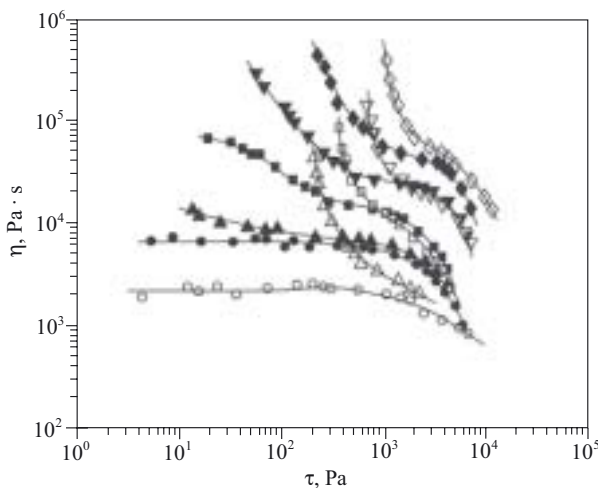


Fig. 8.  $\eta$  vs.  $\tau$  curves for CF/PE-1 (open symbols) and CF/PP-1 (solid symbols) samples with content of CF (in vol. %):  $\circ, \bullet$  — 0,  $\triangle, \blacktriangle$  — 5,  $\square, \blacksquare$  — 10,  $\nabla, \blacktriangledown$  — 15,  $\diamond, \blacklozenge$  — 20

ferent fibre content. As can be seen, highly loaded samples show drastic decrease in  $\eta$  with a small change of  $\tau$ , which indicates yield stresses. For CF/PP-1 systems the existence of high yield stress may be limited to highly loaded systems, and the magnitude of yield stress is smaller than that of CF/PE-1 system with the same fibre content.

So far, many researchers have investigated the factors affecting the relative viscosity ( $\eta_r$ ) of particle-filled systems theoretically and experimentally, but not so many studies exist for fibre-filled systems. Kitano *et al.* [2] suggest the following equation for shear stress-based  $\eta_r$  for fibre-filled systems:

$$\eta_r = \left(1 - \frac{\Phi}{A}\right)^{-2} \quad (1)$$

where:  $A$  — parameter corresponding to the maximum packing, which is determined experimentally, and is expressed as  $A = a - b \cdot a_r$  for systems filled with fibres which aspect ratio ( $a_r$ ), is less than around 50, and  $a$  and  $b$  are constants.

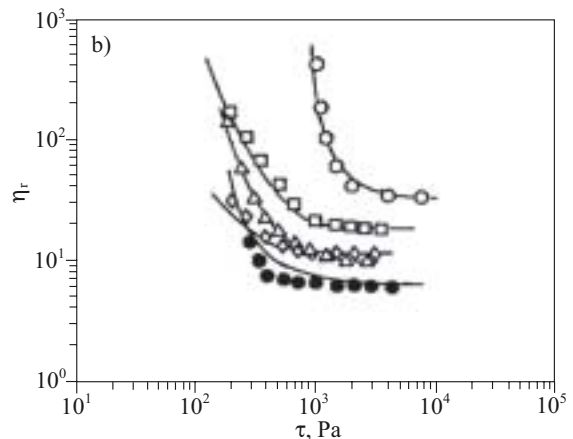
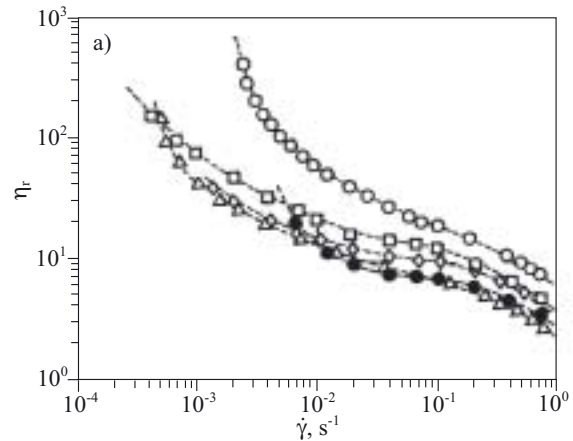


Fig. 9. Relative viscosity ( $\eta_r$ ) of CF-filled polymer samples vs.  $\dot{\gamma}$  (a) and vs.  $\tau$  (b):  $\circ$  — CF20/PE-1,  $\bullet$  — CF20/PE-2,  $\triangle$  — CF20/PP-1,  $\diamond$  — CF20/PP-2,  $\square$  — CF20/PP-3

Figure 9 shows dependence of  $\eta_r$  on  $\dot{\gamma}$  (a) and  $\tau$  (b) for the highest contents (CF20) of filler in all five tested matrices. The former  $\eta_r$  is defined as the ratio of the viscosity of the filled system to that of matrix polymer at the same  $\dot{\gamma}$  value, and the latter is defined at the same  $\tau$ . Values of  $\eta_r$  decrease monotonously with increasing  $\dot{\gamma}$ , and the curves have no plateau. On the other hand,  $\eta_r$  shows nearly constant values in a broad  $\tau$  region, even for the samples with high fibre loading. Except for CF20/PE-1, for all the other presented materials a constant value of  $\eta_r$  can be obtained easily within the attainable  $\tau$ . The figure also shows that the flow curves of fibre-filled systems are influenced not only by fibre characteristics, such as fibre content, fibre length and its distribution, but also the flow properties of the matrix polymer are important.

In order to determine the yield stress of filled systems conventionally, Casson plots are employed. They give

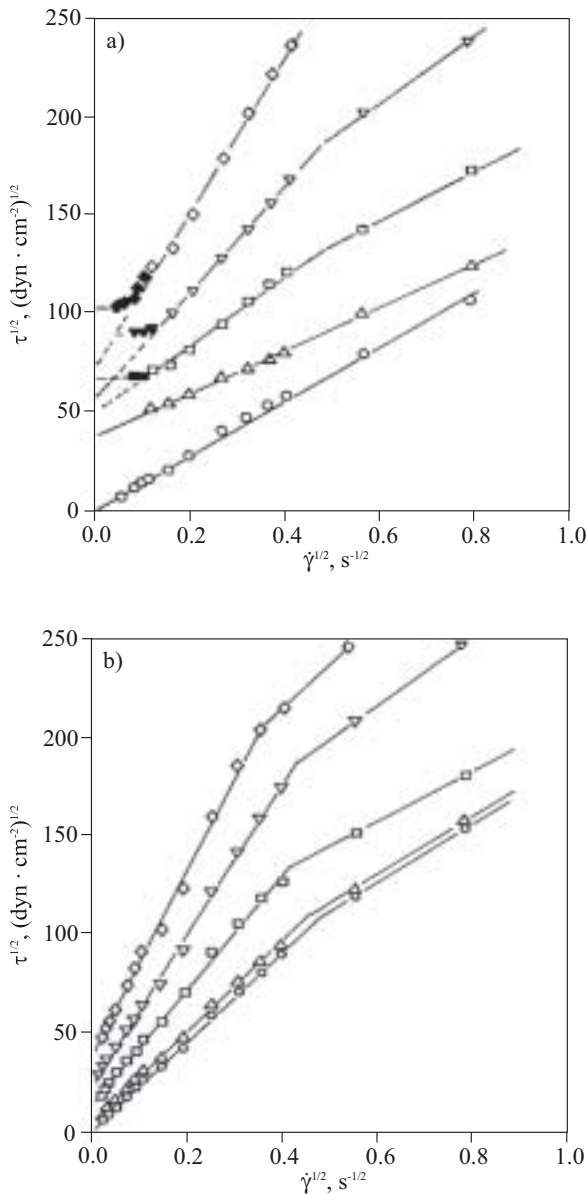


Fig. 10. The Casson plots of CF/PE-1 (a) and CF/PP-1 (b) samples for different content of CF (in vol. %):  $\circ$  — 0,  $\triangle$  — 5,  $\square$  — 10,  $\nabla$  — 15,  $\diamond$  — 20; solid and open symbols represent the data obtained according to procedure A and B, respectively

the relation between the square roots of  $\tau$  and  $\dot{\gamma}$  in the region of low  $\dot{\gamma}$ . Example of Casson plots for CF-filled polymer samples are given in Figure 10.

The data obtained for CF/PE-1 in procedure A (stable  $\tau$  after transient shear flow under stepwise increase in  $\dot{\gamma}$ , shown in Figure 2) are represented in Fig. 10a by filled symbols. As can be seen, the results are not on the straight lines of  $\sqrt{\tau}$  vs.  $\sqrt{\dot{\gamma}}$ , as it is for the data obtained by procedure B. Similar behavior was observed for CF/PE-2 sample. On the other hand, CF/PP-1 sample (and the other PP-based materials) shown in Fig. 10b produces ordinary figures of the Casson plots. The  $\tau$  value at  $\dot{\gamma} = 0$ , i.e. the yield stress, can be determined from the value where the straight extrapolation line crosses the y-axis.

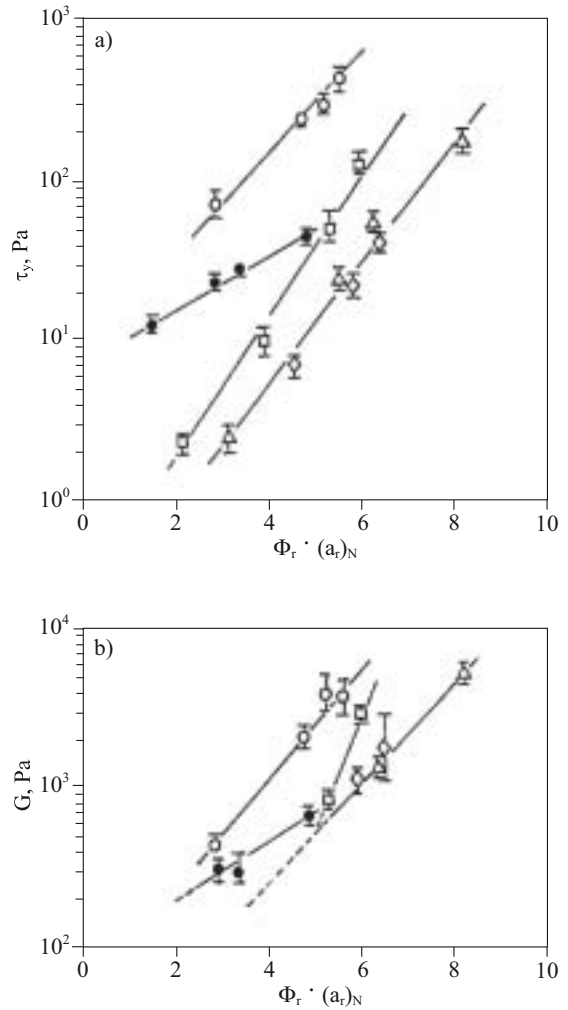


Fig. 11. Yield stress ( $\tau_y$ , a) and shear modulus ( $G$ , b) as functions of product of the volume fraction ( $\Phi$ ) and number average aspect ratio of fibres  $[(a_r)_N]$  for CF-filled polymer systems:  $\circ$  — CF/PE-1,  $\bullet$  — CF/PE-2,  $\triangle$  — CF/PP-1,  $\diamond$  — CF/PP-2,  $\square$  — CF/PP-3

From the constitutive equation of three-dimensionally oriented fibre assemblies discussed in Part I [1]  $\tau$  value of fibre-filled system under simple shear can be presented {from eq. (22) in [1]} as:

$$\tau = C\Phi a_r \Gamma f(\epsilon, \Omega) \tag{2}$$

where:  $C$  — constant determined from the modulus of fibre and its diameter,  $\Gamma$  — value {eq. (13) in [1]} depending on the geometry of fibre assembly and the function of  $\Phi$  and  $a_r$ ,  $f(\epsilon, \Omega)$  — function of deformation (strain,  $\epsilon$ ) and orientation angle distribution under simple shear ( $\Omega$ ).

From eq. (2) the yield stress ( $\tau_y$ ), as one of the special values of  $\tau$ , may be presented as a function of product of  $\Phi$  and  $a_r$ . The relationships between  $\tau_y$  and  $\Phi \cdot (a_r)_N$  values for all the samples measured in the experiments are shown in semi-logarithmic coordinates in Fig. 11a. It can be seen that logarithmic values of  $\tau_y$  are proportional to product  $\Phi \cdot (a_r)_N$  for all samples, therefore  $\tau_y$  can be presented generally by the following empirical exponential equation:

$$\tau_y = A_0 \exp(\Phi \cdot a_r) \quad (3)$$

where:  $A_0$  — material constant depending on the rheological properties of matrix polymer.

Figure 9b also presents (in solid lines) the values of  $\eta_r$  predicted from  $\tau_y$  of each sample and from eqs. (1) and (3) in this paper and eq. (5) in Part I [1] in the form:

$$\eta = A_0 \exp(\Phi \cdot a_r) (\dot{\gamma})^{-1} + \eta_0 \left(1 - \frac{\Phi}{A}\right)^{-2} \left[1 + (\lambda \dot{\gamma})^2\right]^{\frac{(n-1)}{2}} \quad (4)$$

For calculation of  $G$  in the range of low  $\varepsilon$  (before shear flow occurs), eq. (28) or eq. (39) described in [1] for fibre assembly may be applied, and it can be presented as a function of  $\Phi \cdot a_r$ , product the same as for  $\tau/\tau_y$ . Figure 11b shows  $G$ , determined from the slopes of  $\tau$  vs.  $\varepsilon$  curves, in dependence on  $\Phi \cdot (a_r)_N$  (procedure A). Similar results are obtained as in the previous case, so analogically, the dependence can be expressed as:

$$G = B_0 \exp(\Phi a_r) \quad (5)$$

where:  $B_0$  — material constants, which depends on the rheological properties of matrix polymers.

From the previous it can be said that fibre orientation in composite melt is very important because it largely influences the flow properties of the filled systems. In our study we investigated, with the help of optical microphotography, morphological changes of fibre assemblies in the matrix polymer before and after shear flow. The samples were obtained by taking out fast-cooled material after shear flow in several positions between the cone and plate, and they showed change of fibre orientation parallel and perpendicular to the shear direction. The results showed that the effect of low  $\dot{\gamma}$  on the structure changes is negligible for all materials tested; however, at higher  $\dot{\gamma}$  ( $0.0016 \text{ s}^{-1}$  and  $2.25 \text{ s}^{-1}$ ) the samples with low fibre content showed the tendency of fibres to orient in the flow direction, and this orientation increased with rising shear rate and flow time.

## CONCLUSION

The research was focused on the rheological properties of short carbon fibre-filled polyolefin melts (two types of PE and three types of PP) at low shear rates. The morphological changes caused by shear flow have also been investigated. The results can be summarized as follows:

— The tested materials differ in the presence of yield stress at slow shear deformation. While PE-based composites show the yield points at nearly constant strain, PP series has no yield points, even for highly loaded systems. This was observed at the measurements in both cone-plate and parallel-plate rheometers.

— The yield stress and shear modulus of the fibre-filled systems can be determined from the measurements of flow behavior at very low shear rates. Both values can be expressed as exponential functions of the volume fraction and aspect ratio of fibre, and pre-exponential factors depend on the flow properties of matrix polymer.

— The relative viscosity of fibre-filled polymer systems determined at constant shear stress depends on the volume fraction and aspect ratio of fibre through the relation suggested in eq. (1).

— The shear viscosity of fibre-filled systems having the yield stress seems to be presented as using eq. (4).

— The friction effect of fibres on the flow in the narrow gap between cone and plate seems to be negligible. Optical observations proved that the degree of fibre orientation under flow in the rheometer increased with the rise of shear rate.

The research has been a first attempt to predict some rheological properties of filled polyolefins at low shear rate from the volume fraction and aspect ratio of fibres, along with the flow properties of the matrix. More accurate study on a larger series of materials, however, is still to be done.

## ACKNOWLEDGMENT

The authors wish to acknowledge the financial support of the Ministry of Education of the Czech Republic through grant No. MSM 7088352101.

## REFERENCES

1. Hausnerova B., Honkova N., Lengalova A., Kitano T., Saha P.: *Polimery* 2008, 53, Nr 7—8.
2. Kitano T., Funabashi M., Klason C., Kubat J.: *Int. Polym. Proc.* 1988, 3, 67.
3. Araki K., Kitano K., Tateshima T., Lengalova A., Saha P.: *Polym. Polym. Comp.* 2003, 11, 383.
4. Kitano T., Funabashi M.: *Rheol. Acta* 1986, 25, 607.

Received 2 V 2007.